

# An Adaptive Two-level Filtering Technique for Noise Lines in Video Images

**Baris Baykant ALAGOZ**

*Department of Electrical and Electronics Engineering,  
Inonu University, Malatya, Turkey*

*baykant.alagoz@inonu.edu.tr*

**Mehmet Emin TAGLUK**

*Department of Electrical and Electronics Engineering,  
Inonu University, Malatya, Turkey*

*mehmet.tagluk@inonu.edu.tr*

---

## Abstract

Due to narrow-band noise signals in transmission channels, visible lines of disturbance can appear in video images. In this paper, an adaptive method based on two-level filtering is proposed to enhance the visual quality of such images. In the first level, an adaptive orientation selective filter detects and clears the noisy lines in the image. In the second level, a median filter repairs defects resulting from the orientation selective filtering process and also filters the wide-band impulsive noise. It was observed that in case of periodic noisy lines in TV images, this filtering technique can sufficiently enhance the image quality and improve the SNR level.

**Keywords:** Adaptive noise filter, Wireless video image enhancement.

---

## 1. INTRODUCTION

In long distance wireless video transmission systems, periodic noise line patterns commonly appear on the received image. Such noise line patterns in wireless transmission are mostly caused from long-term narrow-band signal interference to the communication channel. In many cases, such interference of by noise signals in the channel is unavoidable and therefore the removal of these noise signals has to be carried out on the received image by using filtering techniques. A basic notch reject filter has been applied for the removal of the noise lines on the images received from the long-distance space missions [1]. Nowadays, with increasing usage of wireless video transmission systems in day-to-day applications there is an increasing demand to develop such filtering techniques to work on received images.

In practice, unlicensed transmitter interference, noise in electronics, multi-path effects, loss of horizontal or vertical synchronization are all seen to cause periodic noise lines on the received image. These noise lines can severely mislead computer vision algorithms employed in autonomous remote control systems used in unmanned vehicles [2-5].

Periodic noise lines in images are commonly seen in imaging systems, which use a row scanning mechanism in the construction of the image data when a long-term noise signal affects the system. For example, mechanical and acoustic vibrations in force sensors were seen to decrease the signal to noise ratio (SNR) of images scanned by an Atomic Force Microscope (AFM) at video rate [6].

In the image enhancement field, a variety of methods have been developed to filter out the effects of random noise on images. Most of these studies have been focused on preserving singular features of the image such as edges, while smoothing other segments of the image [7-11]. Alternatively a nonlinear adaptive filter based on a neural network has been proposed for reducing the additive noise [12]. Many adaptive image restoration methods that analyse the noise and optimise the behaviour of the filter to improve overall filtering performance [13-15]. Specifically, for digital TVs the filters compromise edge detection, and an automated modification of filter coefficients has been addressed in detail by Chan et al. [7, 10]. These filters were mainly

developed to deal with random additive noise in images. In their mathematical formulation, the received signal has been defined as:

$$u_r(x) = u(x) + n(x), \tag{1}$$

where,  $n(x)$  is the random noise and  $u(x)$  is the original noise-free image. Due to the fact that the noise components are treated as a part of the image signal  $u(x)$ , such filters designed for removing random noise are not able to effectively deal with narrow-band noise lines.

In our study, we assume that the received signal has a narrow-band noise signal besides a random noise signal. Under this assumption, a noise signal can be modelled as:

$$u_r(x) = u(x) + n_n(x) + n(x) \tag{2}$$

where,  $n_n(x)$  represents the narrow-band noise.

To enhance the received image coming from highly noisy channel modelled by equation (2), we proposed a filtering structure which is composed of a frequency domain orientation selective notch reject filter for the elimination of the narrow-band noise ( $n_n(x)$ ) [1, 16] and a spatial median filter for impulsive noise [8]. The block diagram of such a two-level filtering is presented in Figure 1.

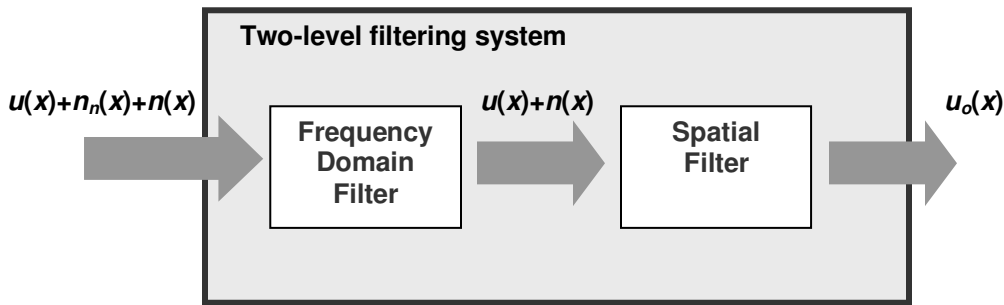


**FIGURE 1:** Block diagram of two-level filtering.

A noisy image is first transformed to red, green and blue color channels, each color channels being solely filtered by the two-level filter designed. In order to adapt the angle of notch reject band to the slope of the noise lines in the received images, the proposed orientation selective filter first detects the spectral region belonging to noise lines, via measuring the local spectral power density, and then it orients the reject band onto the region where the power of noise lines is intensified.

## 2. PROPOSED METHOD

Frequency domain filtering [16] usually provides a good performance in the filtering of narrow-band noise signals, because of allow us eliminating frequency components in a narrow frequency band. Basic design methodology of a frequency domain filter is as follows: The spatial two-dimensional image data are first transformed into frequency components via a two-dimensional Fast Fourier Transform (2DFFT) and then a two-dimensional mask is applied to suppress undesired frequency components, and finally an inverse Fast Fourier Transform (2DIFFT) is used to obtain the filtered image in the spatial domain, as illustrated in Figure 2.

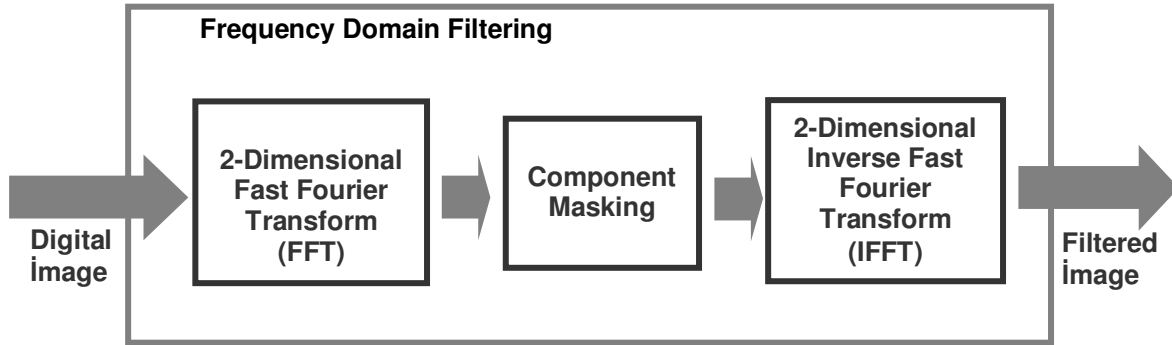


**FIGURE 2.** Frequency domain filtering with component masking

Masking is done by multiplication of each mask element with elements of  $R$ ,  $G$  and  $B$  image as follows:

$$\begin{aligned}
 R_{fm}(u, v) &= R_f(u, v) \cdot Mk(u, v), \\
 G_{fm}(u, v) &= G_f(u, v) \cdot Mk(u, v), \\
 B_{fm}(u, v) &= B_f(u, v) \cdot Mk(u, v),
 \end{aligned}
 \tag{3}$$

where,  $R_f$ ,  $G_f$  and  $B_f$  are the FFT of the  $R$ ,  $G$  and  $B$  matrix,  $R_{fm}$  and  $G_{fm}$  and  $B_{fm}$  are the masked frequency components of the RGB image. The mask matrix  $Mk$  has real value,  $Mk(u, v) \in R$ , in such cases this mask takes effect on the amplitude of the spectral components of images. The phases of frequency components are preserved in this masking operation.

In this study, we introduce a mask  $Mk_\phi$  generation function that provides a directional stop-band over high frequencies to suppress periodic line patterns in the image for a given  $\phi$  angle. The proposed mask is formed from superposition a suppressing channel passing through the origin of the 2D spectrum and a directional pass band at the origin.

The construction of the mask is as follows. The suppressing channel, whose direction is controlled by a given angle,  $\phi$ , was constructed on a base line passing through the origin

$(\frac{M}{2}, \frac{N}{2})$  as presented in Figure 3.

$$u = -\tan(\phi) \cdot (v - \frac{N}{2}) + \frac{M}{2},
 \tag{4}$$

where  $M$  and  $N$  determine the size of the mask,  $Mk_\phi$ , and  $\phi$  is angle of the base line. The shortest distance of any point  $(u, v)$  to this base line, denoted by  $d_s(u, v, \phi)$ , was derived as:

$$d_s(u, v, \phi) = \begin{cases} \sqrt{(u - u_b(u, v, \phi))^2 + (v - v_b(u, v, \phi))^2} & , 90^\circ < \phi < 270^\circ \\ \left| v - \frac{N}{2} \right| & , \phi = 90^\circ \\ \left| u - \frac{M}{2} \right| & , \phi = 270^\circ \end{cases} \quad (5)$$

where  $(u_b(u, v, \phi), v_b(u, v, \phi))$  is the nearest point of the base line to the point  $(u, v)$  on the mask, and calculated by the following expressions:

$$u_b(u, v, \phi) = \tan(\phi) \cdot \left( v_b(u, v, \phi) - \frac{N}{2} \right) + \frac{M}{2} \quad (6)$$

$$v_b(u, v, \phi) = \frac{\tan^2(\phi) \cdot N + 2 \cdot v - \tan(\phi) \cdot M + 2 \cdot \tan(\phi) \cdot u}{2 \cdot (\tan^2(\phi) + 1)} \quad (7)$$

The shortest distance of any point  $(u, v)$  to the centre of the mask, denoted by  $d_c(u, v)$ , is calculated as:

$$d_c(u, v) = \sqrt{\left(u - \frac{M}{2}\right)^2 + \left(v - \frac{N}{2}\right)^2} \quad (8)$$

The mask generation function is then formed as:

$$Mk_\phi(u, v) = \left(1 - \exp\left(-\frac{d_s(u, v, \phi)}{\alpha_s}\right)\right) + \exp\left(-\frac{d_c(u, v, \phi)}{\alpha_c}\right) \cdot \exp\left(-\frac{d_s(u, v, \phi)}{\alpha_s}\right) \quad (9)$$

or in a more compact form:

$$Mk_\phi(u, v) = 1 + \left(\exp\left(-\frac{d_c(u, v, \phi)}{\alpha_c}\right) - 1\right) \cdot \exp\left(-\frac{d_s(u, v, \phi)}{\alpha_s}\right) \quad (10)$$

where  $\alpha_s$  and  $\alpha_c$  are the standard deviations determining the width of directional suppression channel. These parameters also control smoothness of the transition from the stop to pass band of the filter. This smooth transition consequently eliminates ringing effects appearing around patterns in the image. In Figure 4,  $Mk$  matrix generated for various  $\phi$  are illustrated.

The angle  $\phi$  is adaptively determined in a range of  $[\phi_{\min}, \phi_{\max}]$  by applying the following steps:

Step 1: Calculate  $Pw(\phi)$  for all  $\phi$  angles from  $\phi_{\min}$  to  $\phi_{\max}$ . ( $Pw(\phi)$ , expressed by equation (11), is the average spectral power in the image spectrum that is effected by the suppression channel of  $Mk_\phi$ )

Step 2: Use the  $Mk_\phi$  mask in filtering for the  $\phi$ , at which  $Pw(\phi)$  is a maximum and value of this maximum exceeds a predefined filter activation threshold ( $P_{th}$ ). In the case, all  $Pw(\phi) \in [\phi_{\min}, \phi_{\max}]$  are lower than  $P_{th}$ , the current image can bypass filtering. This implies that the noise lines do not have enough power to activate filtering.

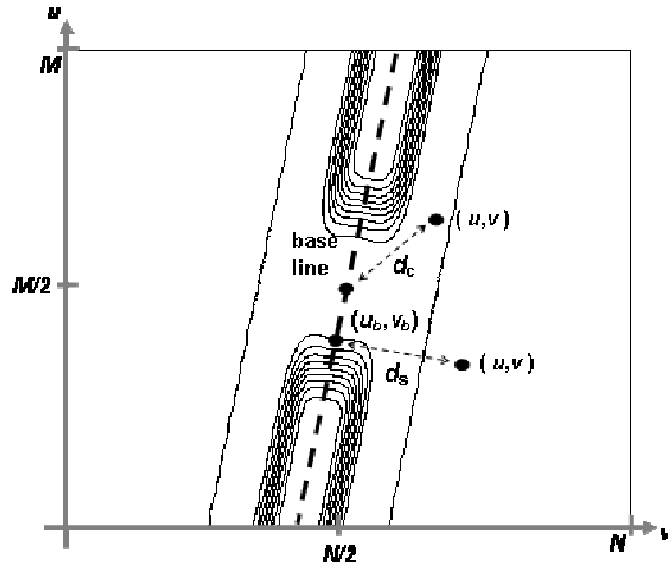


**FIGURE 3.** A contour plot of a suppression channel and its relevant parameters with respect to a base line passing through the centre of the spectrum.

The average image power in the suppression channel  $P_w(\phi)$  can be calculated by:

$$P_w(\phi) = \frac{1}{\sum_{u=0}^{M-1} \sum_{v=0}^{N-1} (1 - Mk(u, v, \phi))} \sum_{u=0}^{M-1} \sum_{v=0}^{N-1} (1 - Mk(u, v, \phi)) \cdot (|R_f(u, v)|^2 + |G_f(u, v)|^2 + |B_f(u, v)|^2) \quad (11)$$

The term  $(1 - Mk(u, v, \phi))$  in equation (11) is the weighting function for spectral components. Equation (11) is a discrete two dimensional extension of a single variable weighted average spectral power given as:

$$P_w = \frac{1}{\int w(f) df} \int w(f) \cdot |I(f)|^2 df \quad \text{for a weight function } w(f).$$

The choice of  $\alpha_c$  and  $\alpha_s$  parameters are in fact based on trial and error. However it was observed that, in this particular application, for TV images with a size of 640x480 pixel, then  $\alpha_c = 2828$  and  $\alpha_s = 316$  can give a satisfactory results.

After removing the noise line patterns from the image by adaptive frequency domain filtering, a 3x3 median filter is applied to the image in order to improve the image quality. This median filtering reduces the deformations resulting from the removal of noise line patterns, as well as the impulsive noise on the filtered image.

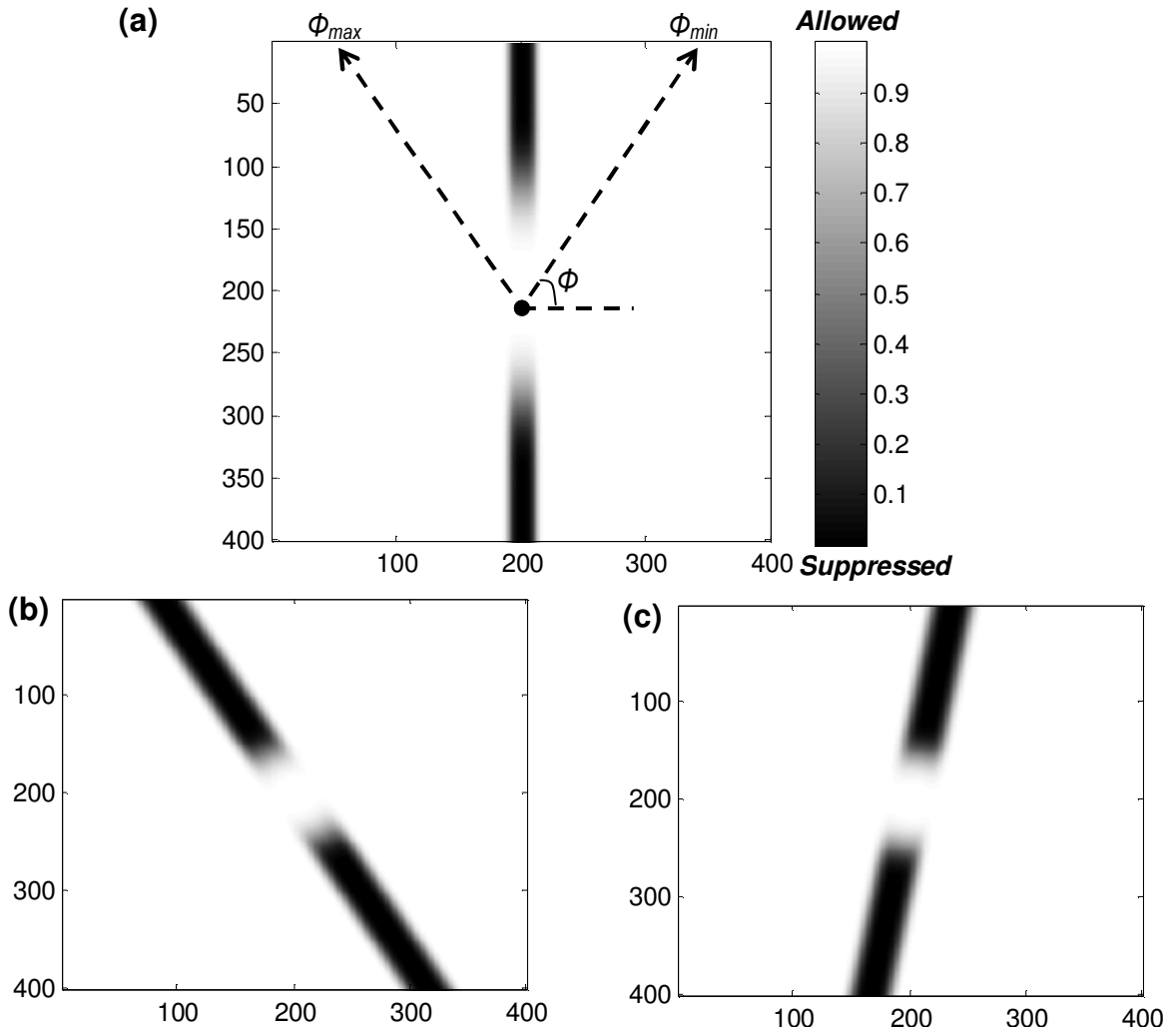


**FIGURE 4.** (a)  $Mk$  matrix generated for  $\phi = 90^0$  (b)  $Mk$  matrix generated for  $\phi = 120^0$  and (c)  $Mk$  matrix generated for  $\phi = 80^0$

### 3. EXPERIMENTAL RESULTS

In Figure 5 and in Figure 6, TV images from a real media broadcast captured by a commercial TV Card were enhanced by the adaptive two-level filtering process described in the previous sections. The calculated spectral power as a function angle  $\phi$  and the resulting  $Mk$  mask are given in the sub-figures (c) and (d), respectively.

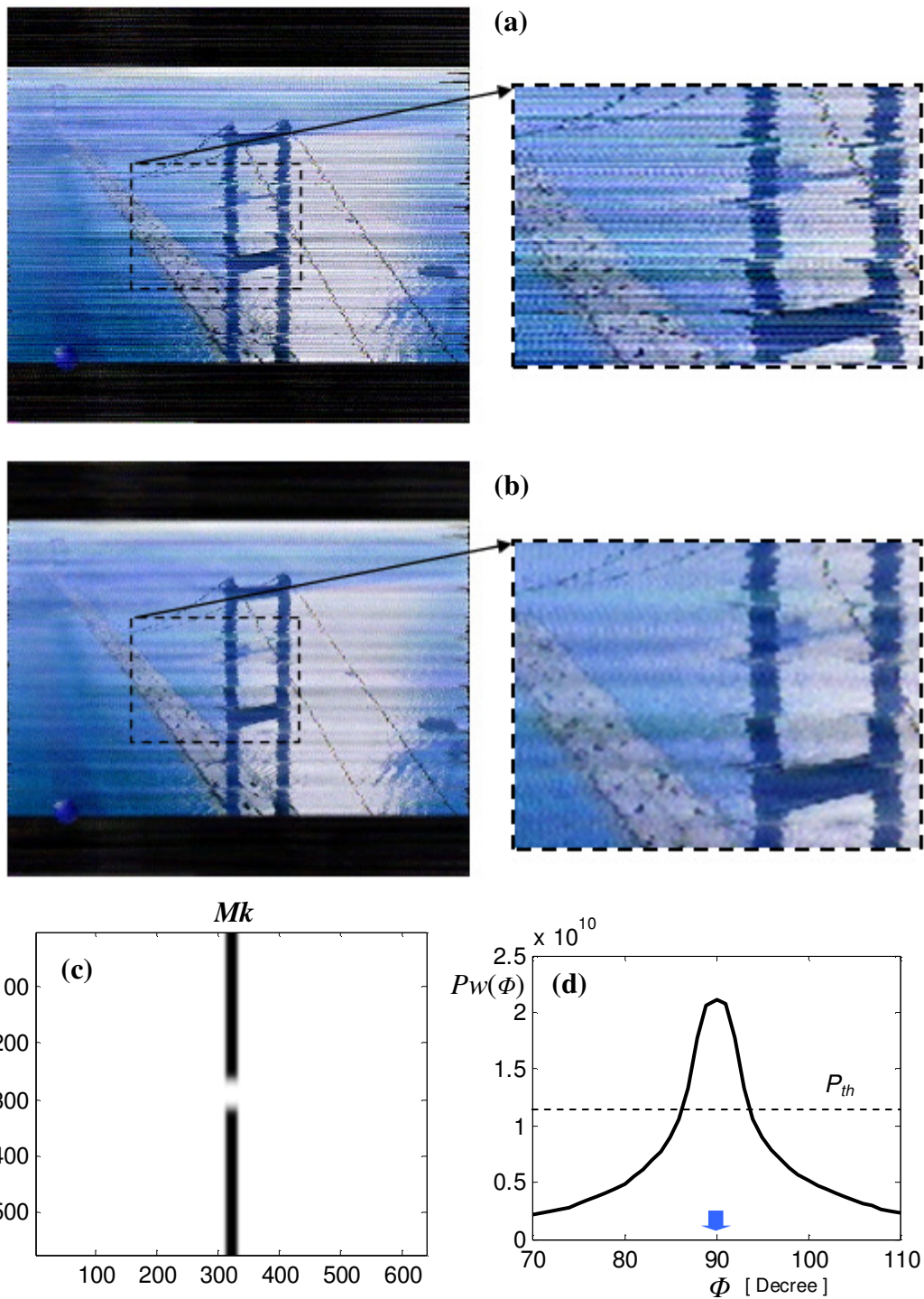


**FIGURE 5.** (a) Noise test image from TV, (b) Enhanced image by filter system ( $\alpha_c = 2828$  ,  $\alpha_s = 316$  ), (c) Generated  $Mk$  matrix, and (d)  $P_w(\phi)$  values in the adaptation process. The filter applied a mask for  $\phi = 90^\circ$  .

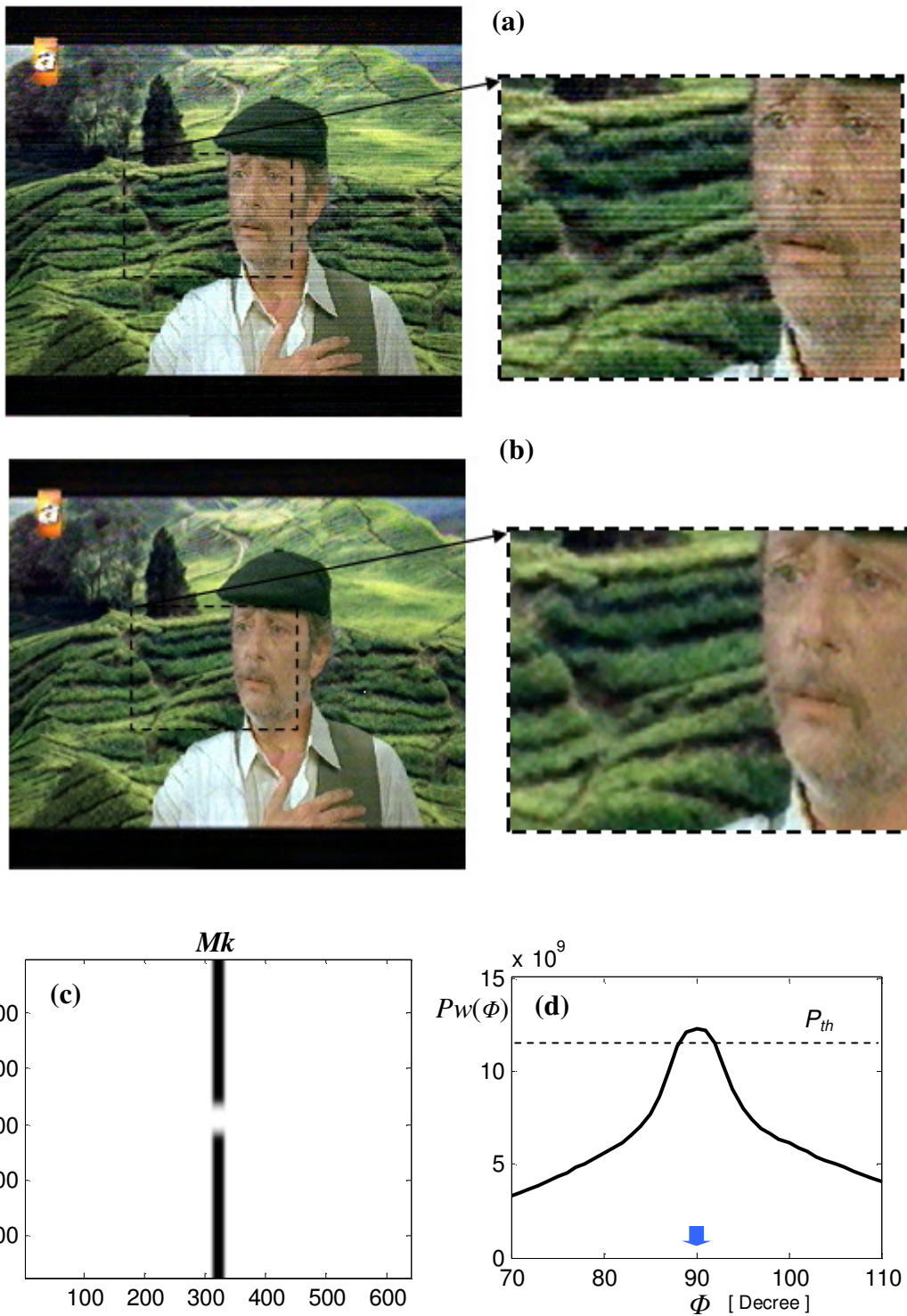


**FIGURE 6.** (a) Noise test image from TV, (b) Enhanced image by filter system ( $\alpha_c = 2828$  ,  $\alpha_s = 316$  ) , (c) Generated  $Mk$  matrix, and (d)  $Pw(\phi)$  values in the adaptation process. The filter applied a mask for  $\phi = 90^0$  .

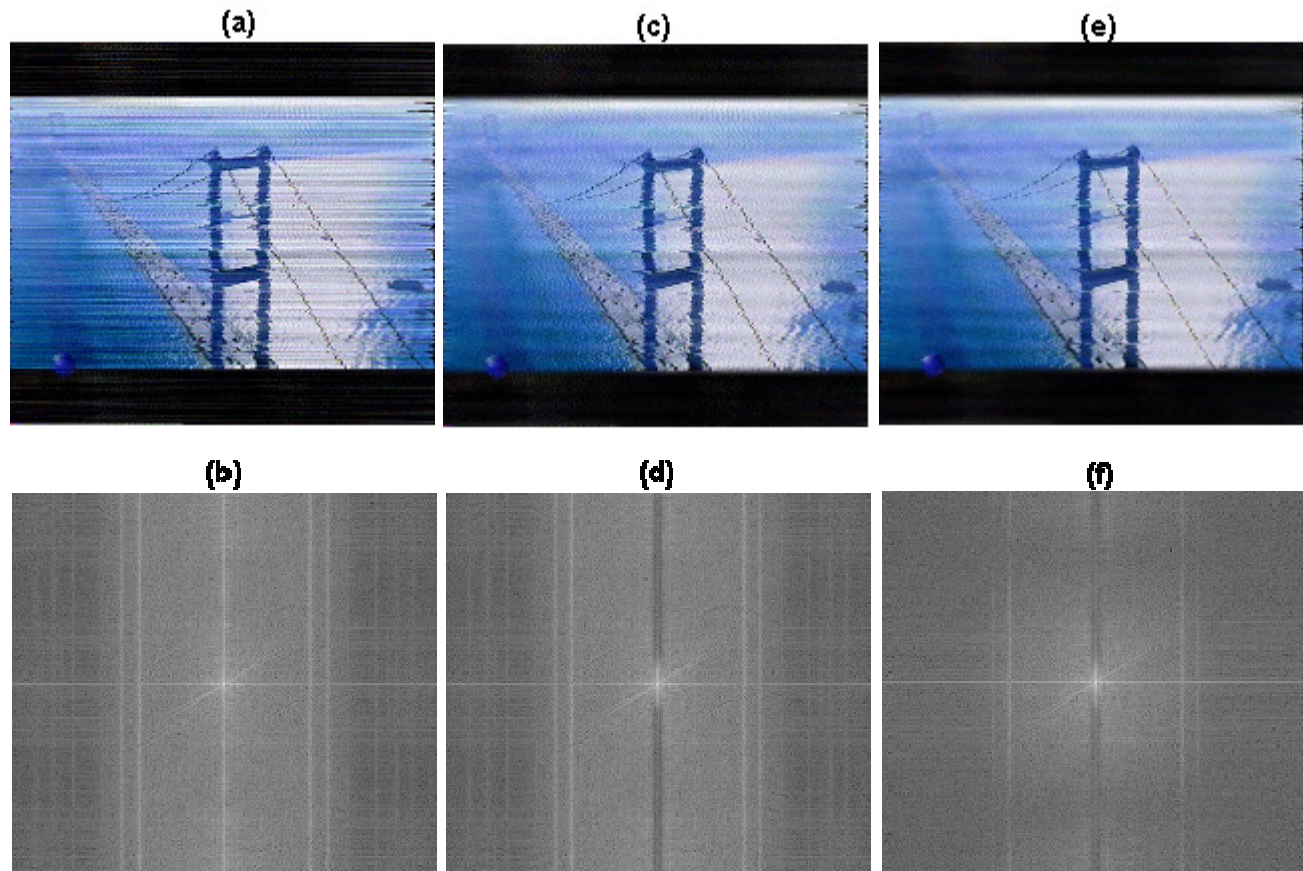


**FIGURE 7.** (a) and (b) are noise test images and their frequency spectrums , (c) and (d) are adaptive orientation selective filtering results and their frequency spectrums , (e) and (f) are median filtered images of (c) and their frequency spectrums..

In Figure 7, the effects of filtering at each level on the test image and its frequency spectrum are illustrated. After cleaning noise line patterns from the image, as seen in Figure 7(c), median filtering with 3x3 windowing can be seen to effectively restore the image from impulsive noise and deformation resulting from the frequency filtering. Median value with respect to image data in 3x3 windows have an effect of repairing notch filtering that is a vertical suppression band passing through the centre in Figure 7(d). This effect can be seen as strengthening some of the frequency components in the vertical suppression band in Figure 7(f).

#### 4. TEST ON SYNTHETIC IMAGE AND SNR LEVELS

In this section, the noisy television test image shown in Figure 8(a) was distorted by a synthetic noise line pattern. This additive noise was generated by a sinusoidal signal with an amplitude of 80 and a frequency set to 0.001, as in Figure 8(c), and a pseudo-random noise signal with a uniform distribution in the interval  $(-50,50)$  , as in Figure 8(d). After adding these noise signals to the television test image in accordance with Equation 2, a noise test image was obtained as shown in Figure 8(b).

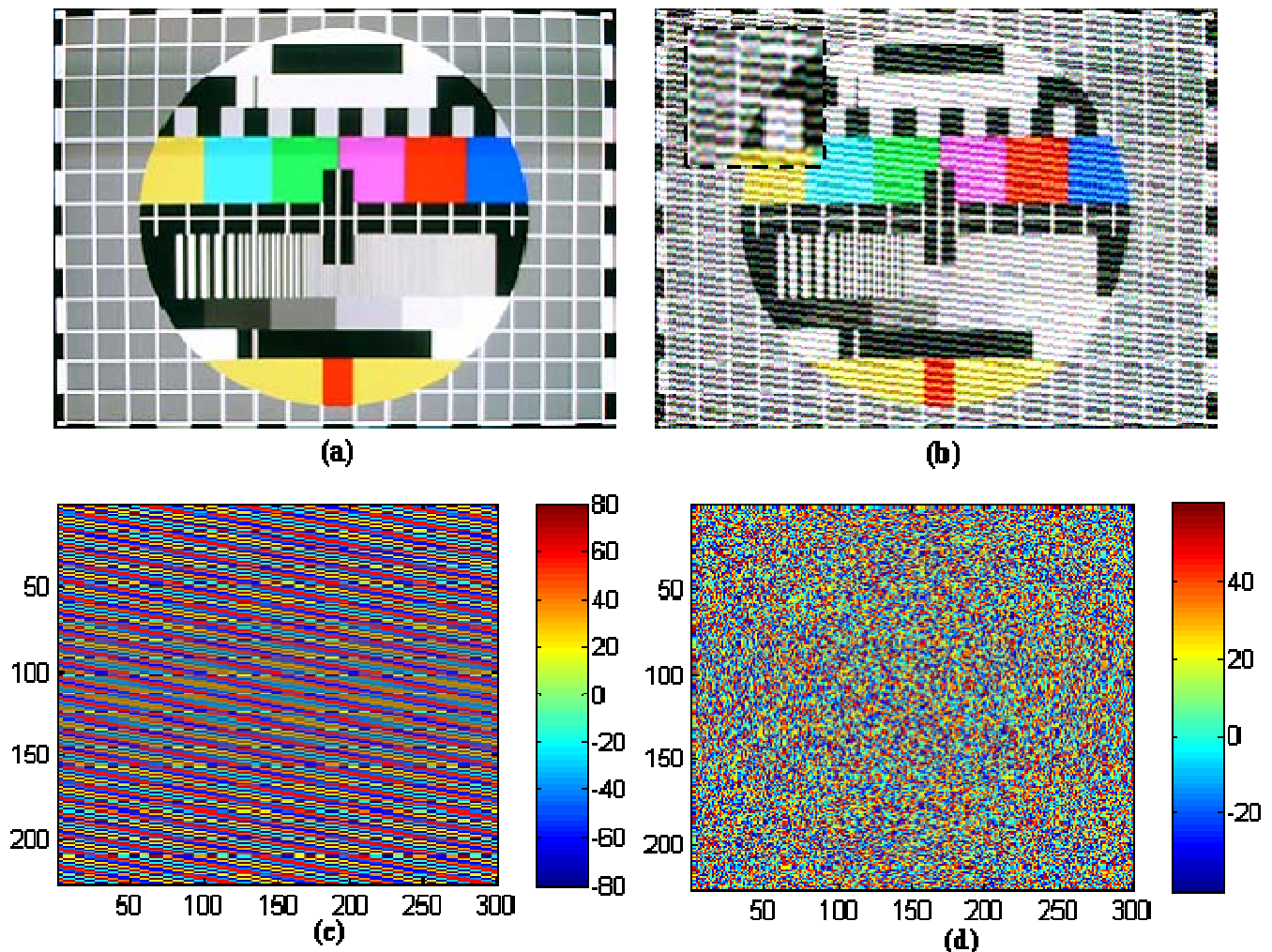


**FIGURE 8.** (a) and (b) are noise test images and their frequency spectrums , (c) and (d) are adaptive orientation selective filtering results and their frequency spectrums , (e) and (f) are median filtered images of (c) and their frequency spectrums.

The noisy television test image given in Figure 8(b) was enhanced by using three different basic filters and the proposed two-level filtering, and the results obtained are demonstrated in Figure 9. In Figure 9 it can be seen that the median-filter and Wiener filter with window size of 3x3 did not sufficiently remove the line patterns in the test image. Even though the Gaussian low pass filter blurred the image, the noise lines are still visible. The proposed method detected the noise lines at  $\phi = 83^0$  and adapted the orientation selective filter according to the noise lines. After the application of both orientation selective filter in the frequency domain and the median filter in the spatial domain the noise lines were removed without too much blurring of the image as seen in Figure 9(d).

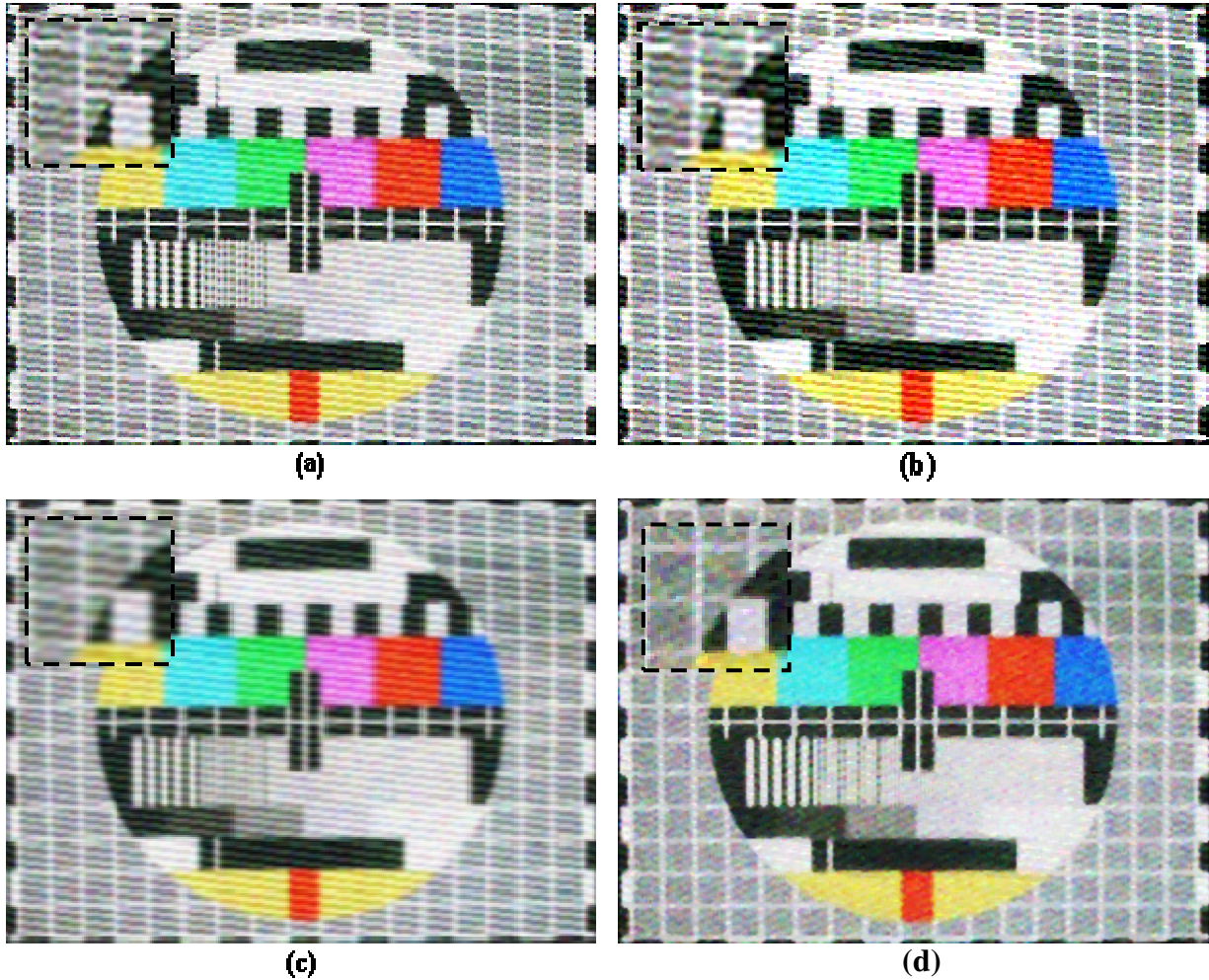


**Figure 9.** (a).Median filtered image, (b) Wiener filtered image, (c) Low pass filtered image by a Gaussian function mask, (d) The proposed two-level filtered image.

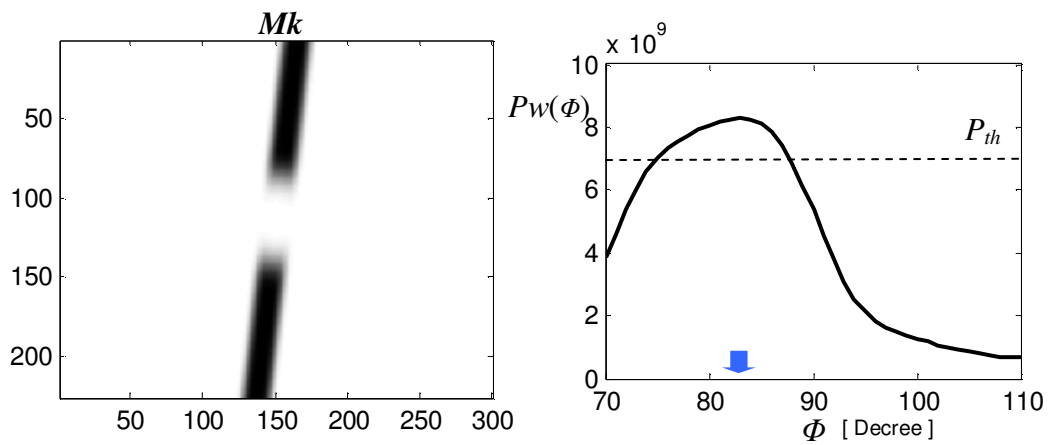


**FIGURE 10.** Generated  $Mk$  matrix and  $Pw(\phi)$  values in the adaptation process. The filter was found to be best when  $\phi = 83^0$ .

In Figure 11, we present Signal to Noise Ratio (SNR) of these filters on the noisy television test image. In these tests, the  $P_{th}$  of the orientation selective filter activation was set to  $3.10^9$ . In this case, when the SNR of the received image is over 40 dB, the noise level remains below  $P_{th}$  and the orientation selective filtering was bypassed and the adaptive two level filtering performed the median filtering on the received image, solely. When the SNR of the test image was decreased to lower levels, the proposed two-level filtering detected the visible noise line patterns in the received image and removed them from the image. In this way, it maintains higher SNRs in the case of a video transmission in highly noisy channel.

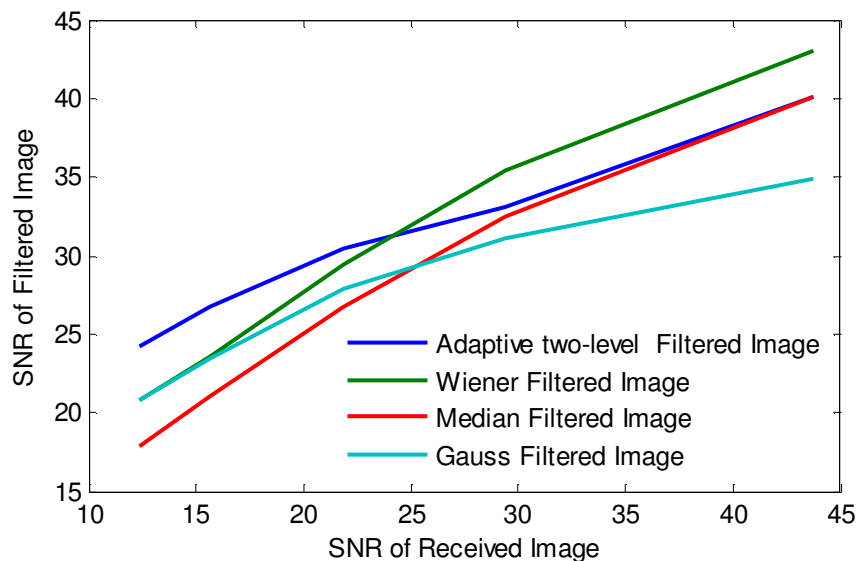


**FIGURE 11.** SNR of the filtered images for various additive noise levels.

## 5. CONCLUSIONS

The noise channel model given by equation (2) provides a more realistic model of today's communication channels. In this manner, a more adaptive and sophisticated filtering system is needed to restore video images. The proposed adaptive two-level filtering method, which integrates an adaptive orientation selective filter and a median filter, was seen to effectively enhance video images containing visible periodic noise lines.

The results obtained show us that the narrow-band noise signal can be detected and filtered by mask adaptive frequency domain filtering and the slight deformations resulting from such frequency domain filtering on the image data can be repaired by the median filtering.

## 6. REFERENCES

- [1] R.C. Gonzalez, R.E. Woods, S.L. Eddins. Digital image processing using MATLAB. New Jersey:Prentice Hall, 2004.
- [2] J. Byrne, R. Mehra." Wireless video noise classification for micro air vehicles." Proceedings of the 2008 Association for Unmanned Vehicle Systems International (AUVSI) Conference, 2008, pp.1-25.

- [3] P.Y. Oh, W.E. Green, G. Barrows. "Flying insect inspired vision for autonomous aerial robot maneuvers in near-earth environments." IEEE International Conference on Robotics and Automation (ICRA) , 2004, pp.2347–2352.
- [4] J. Byrne, M. Cosgrove, R. Mehra. "Stereo based obstacle detection for an unmanned air vehicle." IEEE International Conference on Robotics and Automation (ICRA'06), 2006.
- [5] J. Byrne, C.J. Taylor. "Expansion segmentation for visual collision detection and Estimation." IEEE International Conference on Robotics and Automation Kobe International Conference Center, 2009, pp.875-882.
- [6] G. Schitter, M.J. Rost. "Scanning probe microscopy at video-rate." Materials Today, vol.11, pp.40–48, 2008.
- [7] T.F. Chan, S. Osher, J. Shen. "The digital TV filter and nonlinear denoising." Image Processing IEEE Transaction, vol.10, pp.231-241, 2001.
- [8] C.A. Glasbey, G.W. Horgan. Image analysis for the biological science. Statistics in practice, New York:John Wiley & Sons, 1995.
- [9] B. Jaehne. Digital image processing, Concepts, algorithms, and scientific applications, Berlin:Springer, 1997.
- [10] S. Osher, J. Shen. Digitized PDE method for data restoration, In: G. A. Anastassiou (Ed.), Analytic-computational methods in applied mathematics, Chapman & Hall/CRC, 2000.
- [11] A. Lev, S.W. Zucker, A. Rosenfeld. "Iterative enhancement of noisy images." IEEE Transactions on Systems, Man and Cybernetics, vol.7, pp.435-443, 1977.
- [12] L. Corbalan, G.O. Massa, C. Russo, L. Lanzarini, A. De Giusti. "Image recovery using a new nonlinear adaptive filter based on neural networks." Journal of Computing and Information Technology CIT, vol.14, pp.315–320, 2006.
- [13] H.S. Wong, L. Guan. "A neural learning approach for adaptive image restoration using a fuzzy model-based network architecture." Neural Networks IEEE Transactions, vol.12, pp.516–531, 2001.
- [14] E.S. Hore, B. Qiu, H.R. Wu. "Adaptive noise detection for image restoration with a multiple window configuration." Image Processing Proceedings. 2002 International Conference, 2002, pp. 329-332.
- [15] F. Russo. "A method for estimation and filtering of Gaussian noise in images." Instrumentation and Measurement, IEEE Transactions, vol.52, pp.1148–1154, 2003.
- [16] R.P. Matei. "Design method for orientation-selective CNN filters." Circuits and Systems, Proceedings of the 2004 International Symposium vol.3, 2004, pp.105-8.